the right carotid artery, and a stent was implanted in the injured right FA by balloon inflation (at 12 atm for 20 seconds). Successful stent implantation was confirmed by angiography in all rabbits.

X-Gal stain

For the BMS, gelatin-coated stent, and Lac Z stent groups, β-galactosidase expression in the FA at days 3 and 7 (n=3 in each group, respectively) post stent implantation was quantified with X-Gal stain as previously described[5] to confirm successful gene transfer and protein expression.

Evaluation of Patency of Stent Implanted Arteries

Peak flow velocity in FAs was measured by continuous Doppler method transcutaneously on day 3 post stent implantation (n=10 for the BMS, gelatin-coated stent, and pE-NTPDase stent groups, and n=4 for the Lac Z stent group). Based on differences in peak flow velocity between the stent implanted right FAs and the contralateral normal FAs, we defined differences <30% as patent, > 30% as stenosis, and no flow as occlusion, in accordance with a previous study.[6] Angiography of FAs was carried out to evaluate the patency of the stent implanted arteries on days 3 and 7 post stent implantation (n=10 and 12 on each day for the BMS, gelatin-coated stent, and pE-NTPDase stent groups, n=4 and 6 on each day for the Lac Z stent group). In all rabbits, the stent implanted site of the right FA and the size-matched contralateral normal FA were harvested after angiography for the evaluation of gene and protein expression, NTPDase activity, and histological examination.

RNA Extraction and RT-PCR

In the BMS, gelatin-coated stent, and pE-NTPDase stent groups (n=4), E-NTPDase mRNA expression in whole FAs of stent implanted site, and endothelial nitric oxide

synthase (eNOS) mRNA expression in the neointimal tissues of stent implanted FAs on days 3 and 7 post stent implantation were evaluated by real-time polymerase chain reaction (PCR) as previously described.[7] RNA was isolated from the whole FAs of stent implanted site using TRIzol Reagent (Invitrogen, Carlsbad, CA), after which cDNA was generated from total RNA by using a SuperScript II Reverse Transcriptase Kit (Invitrogen). Real-time polymerase chain reaction (PCR) was then performed in an ABI-Prism 7700 (Applied Biosystems, Foster City, CA) using QuantiTect SYBR Green PCR Kit (Qiagen). The sense and antisense primers were as follows: 5'CATGAATTCCATGGGCAAGGGAACCAAGGACCTGAC3' and 5'AGCACAATCCCATACTTAACG3' for human E-NTPDase, 5'CTACCCCTTTGACTTCCAGGG3' and 5'CTTGGCCAGTTTCTGCCACAG3' for total E-NTPDase including both endogenous rabbit E-NTPDase and exogenous human E-NTPDase, 5'ACCTGTGTGACCCTCACCG3' and 5'GGGGACAGGAAATAGTTGACC3' for eNOS, and 5'GATGACCCAGATCATGTTTG3' and 5'AGGTCCAGACGCAGGATG3' for β-actin. The primers for total E-NTPDase were generated to have high homology to human, rat, and mouse E-NTPDase, because the sequence of rabbit E-NTPDase has not been determined. The mRNA levels of human or total E-NTPDase and eNOS were normalized to β-actin for each sample.

Western Blotting

To evaluate the expression of human pE-NTPDase protein in whole FAs of stent implanted site on days 3 and 7 post stent implantation (n=3 and 4 on each day, respectively, for the BMS, gelatin-coated stent, and pE-NTPDase stent groups), western blotting was performed as previously described[8] with a primary antibody against FLAG (SIGMA-ALDRICH), because there is no specific antibody to human E-NTPDase for western blotting.

Measurement of NTPDase Activity

Rabbit FAs were homogenized in Tris-buffered saline (pH 7.4) containing aprotinin and phenylmethylsulfonyl fluoride. To determine whether human pE-NTPDase protein expressed in the arteries treated with the pE-NTPDase stent exhibited normal enzymatic activity, NTPDase activity was measured by luciferin-luciferase bioluminescence assay using an ATP assay system (TOYO B-Net CO, LTD) on days 3 and 7 post stent implantation (n=3 and 4 on each day, respectively, for the BMS and pE-NTPDase stent groups). Finally, NTPDase activity in the stent implanted FAs was expressed as a ratio to the activity in the contralateral normal FA.

Histological Examination

The stent implanted FAs were fixed in 4% paraformaldehyde. To prepare cross-sections of stent-implanted FAs, fixed arteries were embedded in plastic resin (Technovit 8100, Heraeus Kulzer, Armonk) according to the manufacturer's instructions, separated transversely into 3 parts, and cut into 5 μm sections in each part. Each section was stained with hematoxylin and eosin for histological analysis (n=4 in each group). The sections were also examined immunohistochemically with the antibodies against human pE-NTPDase (YH34)[1,2], α-smooth muscle actin (MCA1906H, AbD Serotec), and macrophages (RAM11, DAKO Japan). Additionally, part of the thrombi in the BMS and gelatin-coated stent groups were extracted, fixed in 4% paraformaldehyde, embedded in paraffin, and cut into 3 μm sections, and immunostaining for GP IIb/IIIa (Affinity Biologicals Inc) was performed.

References

1. Makita K, Shimoyama T, Sakurai Y, Yagi H, Matsumoto M, Narita N, Sakamoto Y, Saito S, Ikeda Y, Suzuki M, Titani K, Fujimura Y. Placental ecto-ATP diphosphohydrolase: its structural feature distinct from CD39, localization and inhibition on shear-induced platelet aggregation. *Int J Hematol*. 1998;68:297-310.
2. Furukoji E, Matsumoto M, Yamashita A, Yagi H, Sakurai Y, Marutsuka K, Hatakeyama K, Morishita K, Fujimura Y, Tamura S, Asada Y. Adenovirus-mediated transfer of human placental ectonucleoside triphosphate diphosphohydrolase to vascular smooth muscle cells suppresses platelet aggregation in vitro and arterial thrombus formation in vivo. *Circulation*. 2005;111:808-815.
3. Fukunaka Y, Iwanaga K, Morimoto K, Kakemi M, Tabata Y. Controlled release of plasmid DNA from cationized gelatin hydrogels based on hydrogel degradation. *J Control Release*. 2002;80:333-343.
4. Kushibiki T, Tomoshige R, Fukunaka Y, Kakemi M, Tabata Y. In vivo release and gene expression of plasmid DNA by hydrogels of gelatin with different cationization extents. *J Control Release*. 2003;90:207-216.
5. George SJ, Lloyd CT, Angelini GD, Newby AC, Baker AH. Inhibition of late vein graft neointima formation in human and porcine models by adenovirus-mediated overexpression of tissue inhibitor of metalloproteinase-3. *Circulation*. 2000;101:296-304.
6. Demchuk AM, Burgin WS, Christou I, Felberg RA, Barber PA, Hill MD, Alexandrov AV. Thrombolysis in brain ischemia (TIBI) transcranial Doppler flow grades predict clinical severity, early recovery, and mortality in patients treated with intravenous tissue plasminogen activator. *Stroke*. 2001;32:89-93.
7. Yoshimoto S, Nakatani K, Iwano M, Asai O, Samejima K, Sakan H, Terada M, Harada K, Akai Y, Shiiki H, Nose M, Saito Y. Elevated levels of fractalkine

expression and accumulation of CD16+ monocytes in glomeruli of active lupus nephritis. *Am J Kidney Dis*. 2007;50:47-58.

8. Kawata H, Yoshida K, Kawamoto A, Kurioka H, Takase E, Sasaki Y, Hatanaka K, Kobayashi M, Ueyama T, Hashimoto T, Dohi K. Ischemic preconditioning upregulates vascular endothelial growth factor mRNA expression and neovascularization via nuclear translocation of protein kinase C epsilon in the rat ischemic myocardium. *Circ Res*. 2001;88:696-704.

Figure legends

Supplemental Figure I

Platelet aggregation induced by ADP (1.0 μg/ml) in rabbit platelet-rich plasma without (A) or with (B) human pE-NTPDase (1.5 μg/ml).

Supplemental Figure II

X-Gal staining of stent implanted FA sections. FAs from the LacZ stent group analyzed on days 3 and 7 exhibited strong X-Gal staining. This was not observed in the BMS or gelatin-coated stent groups.

Supplemental Figure III

Typical images of peak flow velocity at the distal site of stent implantation on day 3. In the BMS, gelatin-coated stent, and LacZ stent groups, the peak flow velocity in the stent implanted FAs is faster than in the contralateral normal FAs in cases of stenosis (A) or undetectable in cases of occlusion (B). In contrast, in the pE-NTPDase stent group, all treated FAs showed blood flow patterns similar to the contralateral normal FAs (C). Dotted lines indicate the peak flow velocity of the contralateral normal FA in each rabbit.

Supplemental Movie I

Representative angiography on day 7 indicating the occlusion of right FA implanted with the stent lacking the pE-NTPDase gene.

Supplemental Movie II

Representative angiography on day 7 showing the patency of right FA implanted with the pE-NTPDase gene-eluting stent.

Supplemental Figure I

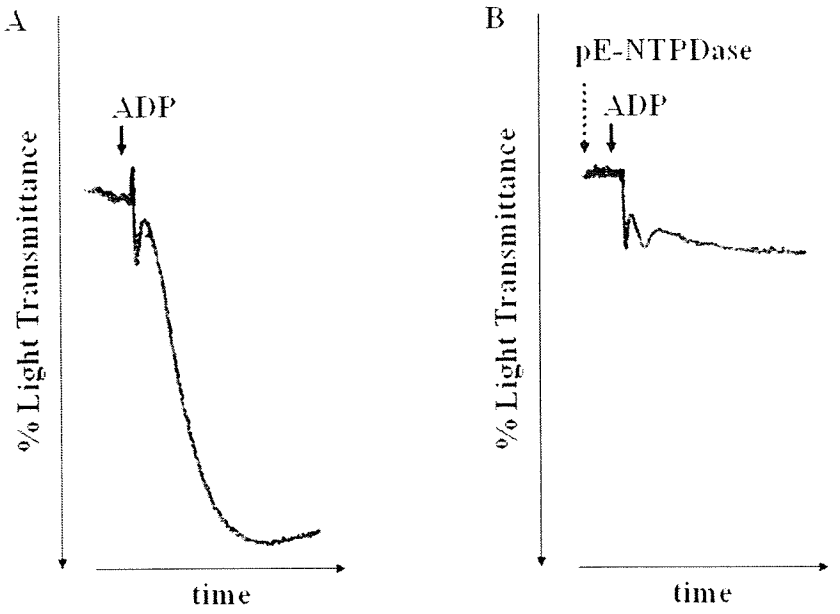

Supplemental Figure II

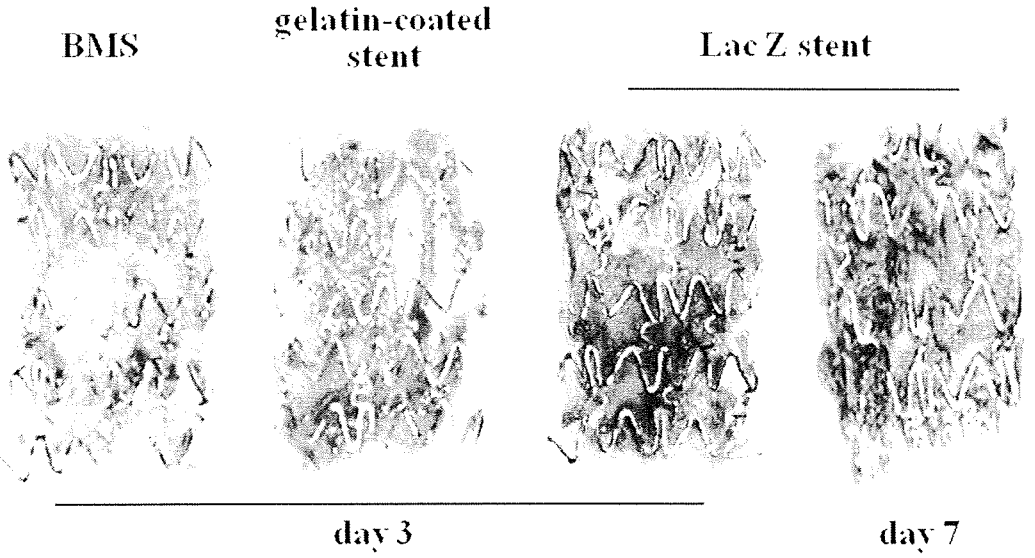

Supplemental Figure III

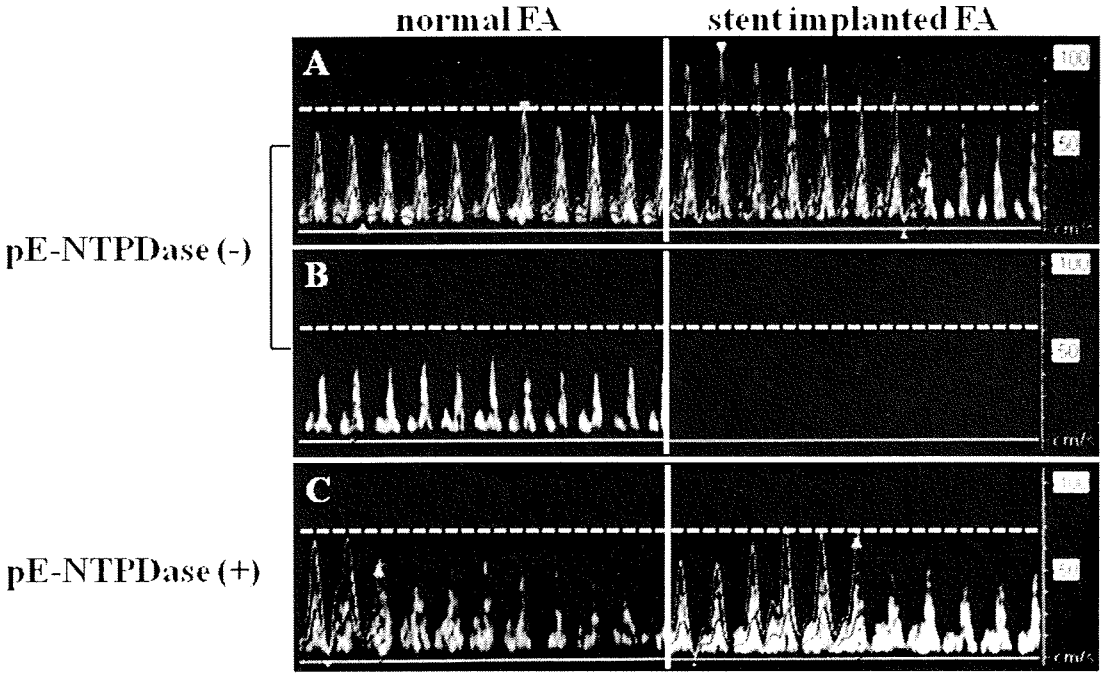

Regulation of Aldosterone and Cortisol Production by the Transcriptional Repressor Neuron Restrictive Silencer Factor

Satoshi Somekawa, Keiichi Imagawa, Noriyuki Naya, Yasuhiro Takemoto, Kenji Onoue, Satoshi Okayama, Yukiji Takeda, Hiroyuki Kawata, Manabu Horii, Tamio Nakajima, Shiro Uemura, Naoki Mochizuki, and Yoshihiko Saito

The First Department of Internal Medicine (S.S., K.I., N.N., Y.Takem., K.O., S.O., Y.Taked., H.K., M.H., T.N., S.U., Y.S.), Nara Medical University, Kashihara, Nara 634-8522, Japan; and Department of Structural Analysis (N.M.), National Cardiovascular Center Research Institute, Suita, Osaka 565-8565, Japan

Aldosterone synthase (CYP11B2) and 11β-hydroxylase (CYP11B1) regulate aldosterone and cortisol production, respectively. The expression of these enzymes is promoted by calcium influx through Cav3.2, a T-type calcium channel. Neuron-restrictive silencer factor (NRSF) binds to neuron-restrictive silencer element (NRSE) to suppress the transcription of NRSE-containing genes. We found a NRSE-like sequence in human CYP11B2 and CYP11B1 genes as well as the CACNA1H gene of many mammalian species. The CACNA1H gene encodes the α-subunit of Cav3.2. Here we investigated how NRSF/NRSE regulates aldosterone and cortisol synthesis. Inhibition of endogenous NRSF by an adenovirus-expressing dominant-negative NRSF (AD/dnNRSF) increased human CYP11B2 and CYP11B1 mRNA expression, leading to aldosterone and cortisol secretion in human adrenocortical (H295R) cells. In reporter gene experiments, NRSE suppressed luciferase reporters driven by CYP11B2 and CYP11B1 promoters and dnNRSF enhanced them. Moreover, cotransfection of dnNRSF increased luciferase activity of reporter genes after deletion or mutation of NRSE, suggesting that NRSF/NRSE regulates transcription of CYP11B2 and CYP11B1 genes indirectly. AD/dnNRSF augmented mRNA expression of rat CYP11B2 and CYP11B1 genes, neither of which contains a NRSE-like sequence in rat adrenal cells. AD/dnNRSE also significantly increased CACNA1H mRNA in H295R and rat adrenal cells. Efonidipine, a T/L-type calcium channel blocker, significantly suppressed dnNRSF-mediated up-regulation of CYP11B2 and CYP11B1 expression. Moreover, NRSF/NRSE is also involved in angiotensin II- and K^+-stimulated augmentation of CYP11B2 and CYP11B1 gene transcription. In conclusion, NRSF/NRSE controls aldosterone and cortisol synthesis by regulating CYP11B2 and CYP11B1 gene transcription mainly through NRSF/NRSE-mediated enhancement of the CACNA1H gene. (***Endocrinology*** **150: 3110–3117, 2009)**

Aldosterone plays a central role in various pathological conditions, including hypertension, heart failure (HF), and postinfarction ventricular remodeling (1, 2). Increased aldosterone or cortisol in HF patients is an independent predictor of mortality risk (3). Thus, understanding the regulation of aldosterone and cortisol synthesis is important for elucidating the mechanisms underlying these disorders. Aldosterone and cortisol are predominantly synthesized and secreted from the adrenal zona glomerulosa and fasciculata, respectively. Aldosterone synthase (CYP11B2) and 11β-hydroxylase (CYP11B1) are responsible for the synthesis of aldosterone (human and rat) and cortisol (human)/corticosterone (rat), respectively (4, 5). Expression of these steroid hydroxylases in the adrenal gland is regulated by angiotensin II (AngII) and extracellular potassium (K^+)-induced calcium influx through calcium channels, particularly Cav3.2, a T-type calcium channel (6–9). These stimuli increase intracellular calcium levels and trigger calcium-calmodulin (CaM)-CaM-dependent protein kinase (CaMK) signaling (10–12). CYP11B2

ISSN Print 0013-7227 ISSN Online 1945-7170
Printed in U.S.A.

doi: 10.1210/en.2008-1624 Received November 18, 2008. Accepted March 26, 2009.
First Published Online April 2, 2009

Abbreviations: AD, Adenovirus; AngII, angiotensin II; CaM, calmodulin; CaMK, CaM-dependent protein kinase; ChIP, chromatin immunoprecipitation; CREB, cAMP response element binding protein; dnNRSF, dominant-negative NRSF; HF, heart failure; K^+, potassium; MOI, multiplicity of infection; NRSE, neuron-restrictive silencer element; NRSF, neuron-restrictive silencer factor; SV40, simian virus 40.

expression is regulated by a number of *cis*-acting transcription factors such as nerve growth factor-induced clone B (13), chicken ovalbumin upstream promoter-transcription factor I (14), cAMP response element binding protein (CREB), and activating transcription factor-1 (15). Moreover, several transcription factors, including CREB, activating transcription factor-1, and steroidogenic factor-1, bind to the 5′-flanking region of the CYP11B1 gene (16, 17). Several of these transcription factors are regulated by calcium-CaM-CaMK signaling. However, the transcriptional regulation of aldosterone and cortisol synthesis remains elusive.

The neuron-restrictive silencer element (NRSE) is a crucial inhibitory DNA element that prevents the expression of neuron-specific genes in nonneuronal and undifferentiated neuronal cells (18). NRSEs are present in a number of neuron-specific genes, including SCG10, the type II sodium channel Nav1.2, and synapsin I (19, 20). The neuron-restrictive silencer factor (NRSF) is a Kruppel-type zinc-finger repressor. NRSF binds to NRSEs, thereby suppressing expression of NRSE-containing genes. Previously we demonstrated that NRSF/NRSE system regulates fetal cardiac gene expression of atrial natriuretic peptides and B-type natriuretic peptides in cultured cardiomyocytes (21, 22).

NRSE-like sequences are found in intron 8 and exon 9 of the human CYP11B2 and CYP11B1 genes. There are no NRSE-like sequences in the rat CYP11B2 and CYP11B1 genes. Moreover, the human and rat CACNA1H genes, which encode the α-subunit of Cav3.2, contain a functional NRSE sequence (23). T-type calcium channels, Cav3.2 in particular, influence aldosterone and cortisol biosynthesis in adrenal cells (9, 24, 25).

We used NCI-H295R, a human adrenocortical cell line (H295R cells), and rat adrenal cells isolated from adrenal glands to analyze how production of aldosterone and cortisol/corticosterone is transcriptionally regulated. We here demonstrate the crucial role of NRSF/NRSE system in the transcriptional regulation of CACNA1H and subsequent induction of CYP11B2 and CYP11B1 in human and rat. This system also directly regulates NRSEs in human CYP11B2 and CYP11B1 genes.

Materials and Methods

Reagents and antibodies

Efonidipine was kindly provided by Nissan Chemical (Tokyo, Japan). Other reagents and antibodies are listed in the supplemental text 1, published as supplemental data on The Endocrine Society's Journals Online web site at http://endo.endojournals.org.

Plasmids and recombinant adenovirus (AD)

Plasmids encoding Myc-tagged dominant-negative NRSF (dnNRSF) were kindly provided by David J. Anderson (California Institute of Technology, Pasadena, CA). The recombinant AD encoding Myc-tagged dnNRSF was purified and concentrated as described previously (21).

Cell culture

The NCI-H295R human adrenocortical cell line (26) was obtained from the American Type Culture Collection (Manassas, VA) and cultured in DMEM/F12 medium containing 2% Ultroser SF (Biosepra, Cergy St. Christophe, France), 1% insulin/transferrin/selenium, penicillin, and streptomycin (9). Cells were maintained at 37 C in a humid atmosphere containing 95% air-5% CO_2.

Rat adrenal cells were obtained from adrenal glands of female Long Evans rats weighing 200–250 g and isolated according to the modified method previously described (27). Briefly, isolation and cell dissociation were performed in MEM (supplemented with penicillin and streptomycin). After a 50-min incubation at 37 C with collagenase (2 mg/ml) and deoxyribonuclease (25 μg/ml), cells were disrupted by gentle aspiration with a sterile pipette, filtered, and centrifuged for 10 min at 100 × g. The cell pellet was then resuspended in OPTI-MEM medium (Invitrogen, Carlsbad, CA) supplemented with 2% fetal bovine serum, penicillin, and streptomycin. This protocol was approved by our institutional review board for animal research.

Both cells were maintained at 37 C under a humid atmosphere of 95% air-5% CO_2.

AD transfection

H295R and rat adrenal cells were cultured in six-well culture dishes at a density of 5×10^5 or 1×10^6 cells/well. One day after H295R cells plating or 2 d after rat adrenal cells plating, each cell was infected with AD/dnNRSF or a control LacZ AD (AD/LacZ) at variety multiplicity of infection (MOI) for 24 h in low-serum medium (DMEM/F12 medium containing 0.1% Ultroser SF or OPTI-MEM medium containing with 0.2% fetal bovine serum). At 24 h after infection, cells were stimulated with the specified drugs for 12 h as indicated in the figures.

Chromatin immunoprecipitation (ChIP) assay

Chromatin from H295R cells was prepared using a ChIP assay kit (Upstate, Charlottesville, VA). The purified chromatin was immunoprecipitated with normal IgG or anti-Myc antibodies or was not treated with antibody (non) 36 h after infection with AD/dnNRSF or AD/LacZ. The immunoprecipitated product was analyzed in PCRs using the following primer pairs: NRSE from the human CYP11B2 gene ($NRSE^{B2}$) ChIP primers, 5′-GTAAGGTGGGGCTGGTCAGAAGT-3′ (forward) and 5′-TCTGAAAGTGAGGAGGGGGGACGT-3′ (reverse); $control^{B2}$ ChIP primers, 5′-GCAAGCAAGAAGACAGTGGAGGG-3′ (forward) and 5′-TGTAGCTCAGGGTTGCTGACCTG-3′ (reverse); NRSE from the human CYP11B1 gene ($NRSE^{B1}$) ChIP primers, 5′-CAGGAATGAAACAGGTTGGAGGC-3′ (forward) and 5′-GAGACGTGATTAGTTGATGGCTC-3′ (reverse); and $control^{B1}$ ChIP primers, 5′-GGCTGTGAATCCATCTGGTCATG-3′ (forward) and 5′-GATAAAGGGGATATCACCACCG-3′ (reverse). Aliquots of chromatin obtained before immunoprecipitation were also analyzed (input).

Reporter constructs

The 1523-bp proximal promoter of the CYP11B2 gene and the 1100-bp proximal promoter of the CYP11B1 gene were described previously (13, 17). These sequences were PCR amplified using a BAC clone as a template (RP11–304E16; BACPAC Resource Center, Oakland, CA). Details are described in the supplemental text 2.

Luciferase assay

For transfection experiments, H295R cells were cultured in 24-well culture dishes at a density of 5×10^4 cells/well and transfected 36 h later. Transfection was performed using 2.0 μl of Lipofectamine (Invitrogen, Carlsbad, CA) and 0.3 μg of reporter plasmid DNA in DMEM/F12 medium for 4 h at 37 C. For cotransfection experiments, various amounts of expression plasmids were included in the transfection reaction; the total amount of DNA was kept constant by adding carrier DNA (empty expression vector). In all experiments, 0.1 μg of pRL-SV40 (Toyo, Tokyo, Japan), an expression plasmid in which the simian virus 40 (SV40) promoter is fused to the Renilla luciferase gene, was cotransfected and used to normalize the luciferase activity. After transfection, cells were incubated in low-serum medium (DMEM/F12 medium containing 0.1% Ultroser SF and antibiotics) for 24 h. Where indicated, transfected cells were stimulated for 12 h. Cells were then lysed and assayed using a luciferase assay

system (Promega, Madison, WI) and a luminometer (TR717; Applied Biosystems, Foster City, CA). In each experiment, cell lysate aliquots from duplicate wells were assayed, and the luciferase activities were normalized to that derived from pRL-SV40 luciferase.

RT-PCR

Total RNA (1 μg) extracted from H295R and rat adrenal cells with Trizol (Invitrogen, Carlsbad, CA) was reverse transcribed with SuperScript II and random primers (Invitrogen). The expression levels of specific mRNAs were measured using SYBR green real-time PCRs (QIAGEN, Valencia, CA) with gene-specific primers (supplemental Table 1). Real-time PCR primers and probes for human CYP11B2, human CYP11B1, human NRSF, rat CYP11B2, and rat CYP11B1 were used for TaqMan probe assays (assay Hs01597732_m1, Hs01596404_m1, Hs00194498_m1, Rn02396730_g1, Rn02607234_g1; Applied Biosystems). RT-PCRs were conducted in an ABI Prism Sequence Detection System 7700 (Applied Biosystems).

Western blot analysis

Details are available in supplemental text 3.

EMSA

Nuclear extract from H295R cells was prepared as previously described (21). Double-stranded oligonucleotides containing two copies of the $NRSE^{B2}$ (5′-GCCTCTGTCCTAGGTGCTGAA-3′), a mutant variant of $NRSE^{B2}$ (5′-GCCTCTGTAATACGTGCTGAA-3′), the $NRSE^{B1}$ (5′-GCTTCTGTCCTAGGTGCTGAA-3′), or a mutant variant of $NRSE^{B1}$ (5′-GCTTCTGTAATACGTGCTGAA-3′) were synthesized and used as probes for EMSAs. DNA-protein binding reactions were carried out in a 20-μl final volume of reaction buffer containing 20 mmol/liter HEPES (pH 7.9), 125 mmol/liter KCl, 5 mmol/liter $MgCl_2$, 10% glycerol, 125 μg/ml polydeoxyinosinic-deoxycytidylic acid, and 1 mmol/liter dithiothreitol. The nuclear extract (15 μg protein) was added to the reaction buffer and preincubated for 10 min on ice. Radiolabeled DNA probe was then added, and the nuclear extract was incubated for another 30 min at room temperature. Samples were separated on a 6% retardation gel (Invitrogen) at 300 V in 0.5× Tris-borate EDTA buffer for 20 min. For competition assays, a 50-fold excess of double-stranded $NRSE^{B2}$, $NRSE^{B1}$, the mutated version of $NRSE^{B2}$, the mutated version of $NRSE^{B1}$, a consensus NRSE, or the CREB sequence (supplemental Table 1) was incubated in reaction mixture with a radiolabeled $NRSE^{B2}$ or $NRSE^{B1}$ probe as described above. NRSF antibodies were used in the gel shift experiment.

RIA and ELISA

Aldosterone and cortisol secretion was assayed as previously described (9). Details are provided in the supplemental text 4.

Statistical analysis

Results are expressed as the means ± SD. Student's *t* tests were used to analyze differences between two groups. Within-group differences and between-group differences after treatments were assessed with one-way ANOVA and two-way ANOVA, respectively. Significant differences were defined as $P < 0.05$.

Results

NRSE-like sequences are present in the human CYP11B2 (hCYP11B2) and CYP11B1 (hCYP11B1) genes

A homology search for NRSE-like sequences identified NRSE-like sequences within the genomic sequence corresponding to intron 8 and exon 9 of the human genes but not in those of other species (supplemental Table 2).

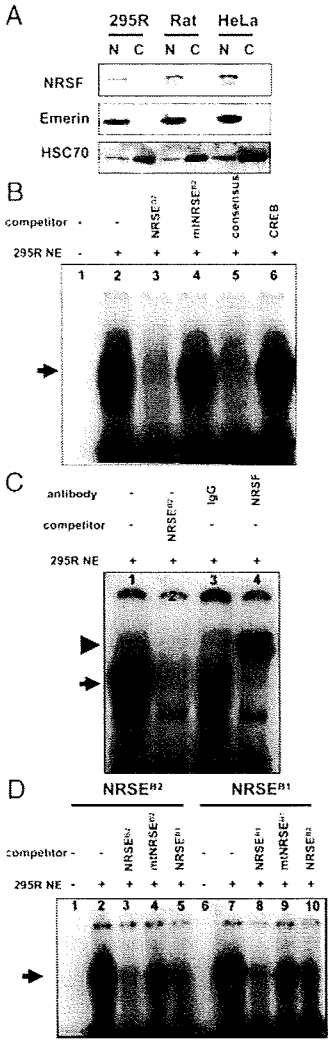

FIG. 1. NRSF binds to NRSEs in the human CYP11B2 ($NRSE^{B2}$) and CYP11B1 ($NRSE^{B1}$) genes in H295R cells. Panel A, Nuclear proteins from H295R and rat adrenal cells were immunoblotted with the antibodies indicated at the *left*. HeLa cells were used as a positive control for NRSF. Emerin and HSC70 were examined as positive controls for nuclear and cytosolic proteins, respectively. N, Nuclear fraction; C, cytosolic fraction. Panels B–D, Nuclear proteins extracted from H295R cells were analyzed by EMSA. Each 15-μg sample of nuclear extract (NE) was incubated with 21-bp double-stranded $NRSE^{B2}$ (panels B, C, and the left side of panel D) and $NRSE^{B1}$ (the right side of panel D) labeled with ^{32}P ATP as a probe. The NRSF antibody and preimmune serum (control) were used in a supershift assay to confirm $NRSE^{B2}$-specific binding (panel C). Excess unlabeled probe or each mutant NRSE sequence was used as cold competitor as indicated. The positions of NRSF-DNA and NRSF-DNA-antibody complexes are indicated with *arrows* and an *arrowhead*, respectively.

NRSF binds to the NRSEs in the hCYP11B2 and hCYP11B1 genes in H295R cells

Western blots showed that NRSF was localized in the nuclei of H295R and primary rat adrenal cells in a manner similar to that observed in HeLa cells, which express NRSF abundantly (Fig. 1A). To test whether the NRSF binds to the NRSEs in hCYP11B2 ($NRSE^{B2}$) and hCYP11B1 ($NRSE^{B1}$) genes, we performed an EMSA with nuclear extracts from H295R cells. A shifted band was observed when the putative $NRSE^{B2}$ sequence was used as the radiolabeled probe (Fig. 1, B and D, lane 2). No band shift was detected when the binding reaction included excess molar amounts of unlabeled $NRSE^{B2}$ (Fig. 1, B and D, lane

3), consensus NRSE (Fig. 1B, lane 5), or NRSE^{B1} (Fig. 1D, lane 5). In contrast, unlabeled probe corresponding to mutated NRSE^{B2} (Fig. 1, B and D, lane 4) or CREB-binding sequences (Fig. 1B, lane 6) had no effect on the band shift. In addition, the band was supershifted in reactions containing antibodies specific for NRSF (Fig. 1C, lane 4, *arrowhead*). We obtained similar results using radiolabeled NRSE^{B1} probe (Fig. 1D, lanes 7–10). As shown in the EMSA, NRSF binds to both NRSEs.

NRSE functions in the hCYP11B2 and hCYP11B1 genes in H295R cells

To test whether the NRSF/NRSE system regulates aldosterone and cortisol biosynthesis in H295R cells, we examined the effects of dnNRSF, which is lacking the repressor domain but still contains the DNA-binding domain (28). Aldosterone and cortisol secretion in human cells increased in response to NRSF inhibition with an AD/dnNRSF (Fig. 2, A and B). The mRNA levels of hCYP11B2 and hCYP11B1 were also markedly increased after transfection with AD/dnNRSF (Fig. 2, C and D).

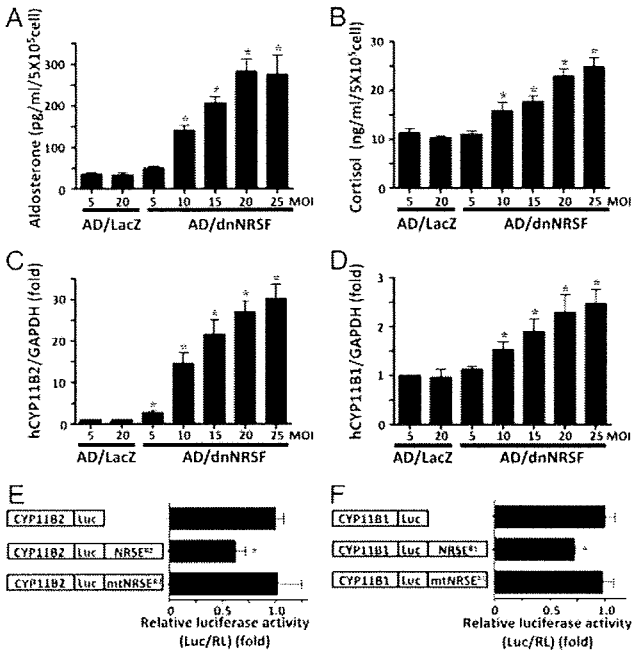

FIG. 2. NRSE regulates hCYP11B2 and hCYP11B1 gene expression in H295R cells. A and B, Effect of inhibiting endogenous NRSF using AD/dnNRSF on aldosterone (A) and cortisol (B) secretion from H295R cells. C and D, hCYP11B2 (C) and hCYP11B1 (D) mRNA were analyzed by quantitative RT-PCR in H295R cells infected with either LacZ AD (AD/LacZ) or AD/dnNRSF. H295R cells were infected with AD/dnNRSF and AD/LacZ at different MOIs as indicated. The expression of each mRNA was normalized to that of glyceraldehyde-3-phosphate dehydrogenase (GAPDH) mRNA. The fold increase of four independent experiments (mean ± SD) relative to that observed in cells infected with AD/LacZ at 20 MOIs is shown in C and D. Statistical significance was analyzed using one-way ANOVA (*, $P < 0.05$ *vs.* 20 MOIs AD/LacZ in A–D). E, H295R cells transfected with the reporter plasmids driven by hCYP11B2 promoter (indicated on the left) together with pRL-SV40 were incubated in low-serum medium for 36 h. Promoter regulation was assessed by firefly and renilla luciferase activities in the cell lysates. The data represent firefly luciferase activity (Luc) normalized to renilla luciferase activity (RL) in each cellular lysate. The mean ± SD of four independent experiments is expressed as the fold increase relative to the luciferase activity of CYP11B2/Luc (control). F, Similar experiments were performed using the hCYP11B1 promoter. Statistical significance was analyzed using one-way ANOVA (E and F). *, $P < 0.05$ *vs.* each control sample.

In a ChIP assay, Myc-tagged dnNRSF bound to NRSE^{B2} and NRSE^{B1} in human cells (supplemental Fig. 1, A and B). Chromatin DNA fragments coimmunoprecipitated by anti-Myc antibodies but not control IgG or no antibody were amplified using primers specific for the NRSEs in hCYP11B2 and hCYP11B1. The coimmunoprecipitated DNA fragment was not amplified by control primers corresponding to 5′-flanking sequences from the hCYP11B2 and hCYP11B1 genes.

To examine whether NRSE^{B2} and NRSE^{B1} function in the transcriptional regulation of hCYP11B2 and hCYP11B1 genes, we constructed a reporter plasmid consisting of the hCYP11B2 or hCYP11B1 promoter and the luciferase gene (CYP11B2/Luc or CYP11B1/Luc) followed by wild-type NRSE^{B2} (CYP11B2/Luc/NRSE^{B2}) or NRSE^{B1} (CYP11B1/Luc/NRSE^{B1}). Plasmids in which wild-type NRSE^{B2} or NRSE^{B1} was replaced with mutated NRSE^{B2} or mutated NRSE^{B1} (CYP11B2/Luc/mtNRSE^{B2} or CYP11B1/Luc/mtNRSE^{B1}, respectively) were also constructed to confirm the functional reliability of NRSE. The luciferase activity of CYP11B2/Luc/NRSE^{B2} was reduced by about 35% compared with that of the control CYP11B2/Luc reporter gene (Fig. 2E). Replacement of NRSE^{B2} with mutated NRSE^{B2} recovered the NRSE-dependent reduction of promoter activity, as demonstrated by comparison of CYP11B2/Luc/NRSE^{B2} and CYP11B2/Luc/mtNRSE^{B2}. Similar results were obtained when CYP11B1/Luc/NRSE^{B1} and CYP11B1/Luc/mtNRSE^{B1} were compared (Fig. 2F). Furthermore, thymidine kinase promoter-dependent gene regulation was inhibited in the presence of either NRSE^{B2} or NRSE^{B1} (supplemental Fig. 2). These results suggest that NRSE^{B2} and NRSE^{B1} function directly in the transcriptional regulation of hCYP11B2 and hCYP11B1 genes in human adrenal cells.

NRSF/NRSE-mediated transcriptional regulation of human CACNA1H (hCACNA1H) is involved in hCYP11B2 and hCYP11B1 expression in H295R cells

To confirm that NRSE^{B2} and NRSE^{B1} suppress hCYP11B2 and hCYP11B1 luciferase activity, respectively, an expression plasmid encoding dnNRSF was cotransfected with the reporter genes. Reporter activity was three times greater in CYP11B2/Luc after dnNRSF expression (Fig. 3A). The effect of dnNRSF on reporter activity in CYP11B2/Luc/NRSE^{B2} was greater than recovery of NRSE-dependent inhibition and was similar to that observed in CYP11B2/Luc (Fig. 3A). Furthermore, dnNRSF affected reporter activity, even in CYP11B2/Luc/mtNRSE^{B2} (Fig. 3A). We observed similar results in the hCYP11B1 promoter-dependent reporter assay (Fig. 3B). These data clearly indicate that the contribution of indirect regulation by NRSF/NRSE system is much greater than direct regulation of hCYP11B2 and hCYP11B1 via NRSE^{B2} and NRSE^{B1}.

We have previously shown that hCACNA1H contains a NRSE (23). The transcriptional product of CACNA1H, Cav3.2, is thought to be involved in aldosterone and cortisol production (9). We hypothesized that indirect regulation of hCYP11B2 and hCYP11B1 genes via T-type calcium channel-mediated (Cav3.2 mediated) calcium-CaM-CaMK contributes to hCYP11B2 and hCYP11B1 expression. To test this hypothesis, we investigated the role of NRSF in transcriptional regulation of the

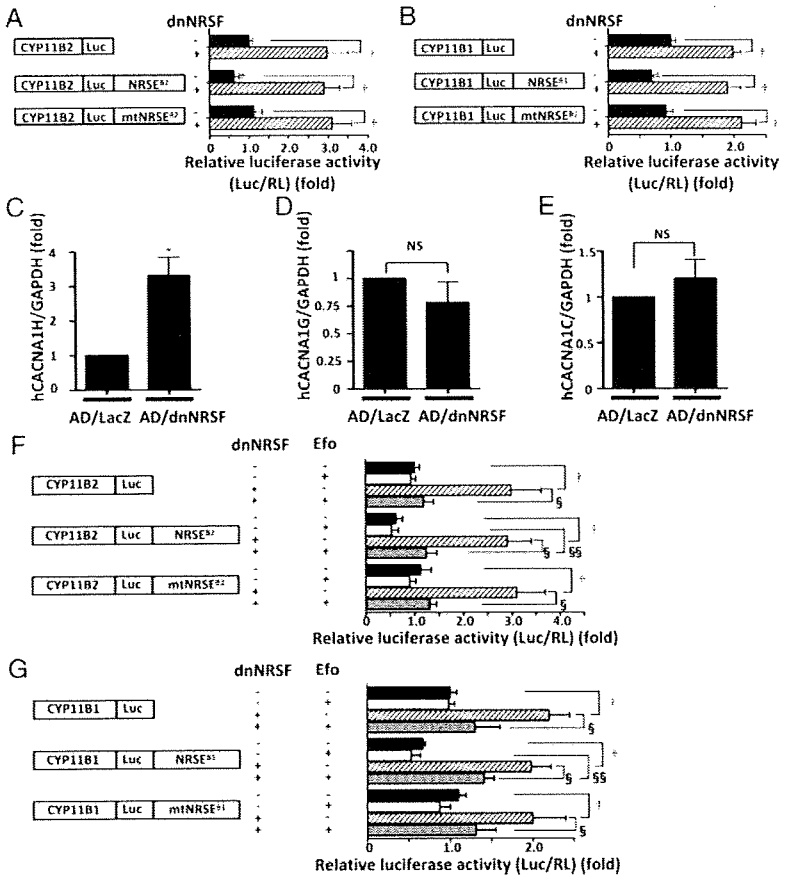

FIG. 3. NRSF/NRSE-mediated transcriptional regulation of hCACNA1H is involved in hCYP11B2 and hCYP11B1 expression in H295R cells. A and B, H295R cells were transfected with the plasmids indicated at the *left* together with dnNRSF or control plasmid. The effect of dnNRSF on the luciferase activity of the hCYP11B2 promoter (A) or the hCYP11B1 promoter (B) was examined as described for Fig. 1E. C–E, The expression of hCACNA1H, hCACNA1G, and hCACNA1C mRNA by forced expression of AD/dnNRSF (20 MOIs) was analyzed by quantitative RT-PCR in H295R cells. AD/LacZ (20 MOIs) was used as a control. The mean ± SD of four independent experiments is expressed as the fold increase relative to the values observed in cells infected with AD/LacZ. Statistical significance was analyzed using Student's *t* test (*, $P < 0.05$). F and G, The effect of efonidipine (Efo), a T/L-type dual calcium channel blocker, on the regulation in dnNRSF-controlled hCYP11B2 (F) and hCYP11B1 (G) promoter activity was tested in H295R cells transfected with the plasmids indicated at the *left*. The cells were treated without (−) or with (+) efonidipine, in low serum medium for 12 h after 24 h of transfection. The data represent firefly luciferase activity (Luc) normalized to renilla luciferase activity (RL) in each cellular lysate. The mean ± SD of six independent experiments is expressed as the fold increase relative to the luciferase activity of CYP11B2/Luc (A and F) and CYP11B1/Luc (B and G). Statistical significance was analyzed using two-way ANOVA. *, $P < 0.05$ *vs.* each control sample; †, $P < 0.05$; §, $P < 0.05$ and §§, $P < 0.05$ between the groups indicated (A, B, F, and G). NS; Not significant.

hCACNA1H gene. hCACNA1H mRNA was up-regulated by AD/dnNRSF in H295 cells (Fig. 3C), but AD/dnNRSF had no effect on human CACNA1G (hCACNA1G) or human CACNA1C (hCACNA1C) mRNA, neither of which contain a NRSE sequence (Fig. 3, D and E). These genes encode the α-subunit of Cav3.1, a T-type calcium channel, and the α-subunit of Cav1.2, an L-type calcium channel, respectively.

To verify the contribution of calcium channel-mediated regulation to dnNRSF-promoted hCYP11B2 and hCYP11B1 expression, we examined the effect of efonidipine, a dual T/L-type calcium channel blocker, on reporter activity in CYP11B2/Luc, CYP11B2/Luc/NRSE^{B2}, and CYP11B2/Luc/mtNRSE^{B2} in the presence and absence of dnNRSF. Efonidipine (0.3 μM) completely inhibited the dnNRSF-induced reporter activity of CYP11B2/Luc and CYP11B2/Luc/mtNRSE^{B2} (Fig. 3F). The promoter activity of CYP11B2/Luc/NRSE^{B2} in response to a combination of dnNRSF and efonidipine was significantly greater than that observed with efonidipine alone (Fig. 3F). These differences indicate that NRSF/NRSE system directly mediates the increase in promoter activity in humans, although, as expected, this effect was smaller than the calcium-mediated effect. Nifedipine (0.3 μM), an L-type calcium channel blocker, did not reduce the dnNRSF-induced activity of the three CYP11B2 promoter reporters (data not shown). Similar results were obtained for hCYP11B1-regulated reporter expression (Fig. 3G). Collectively, these data suggest that NRSF/NRSE mainly regulates the expression of hCYP11B2 and hCYP11B1 in a manner dependent on calcium influx via T-type calcium channels.

Blocking T-type calcium channels inhibits the dnNRSF-induced increases in hCYP11B2 and hCYP11B1 mRNA expression in H295R cells

We assumed that CaMK activation via calcium influx through Cav3.2 might enhance the promoter activity of the hCYP11B2 and hCYP11B1 genes containing upstream *cis* elements responsive to CaMK signaling. Thus, we investigated the effects of efonidipine, nifedipine, and KN93 (a CaMK I, II, and IV inhibitor) on the dnNRSF-induced increase in aldosterone and cortisol secretion and the dnNRSF-regulation of hCYP11B2 and hCYP11B1 mRNA expression in H295R cells. Increased aldosterone and cortisol secretion was suppressed by either efonidipine or KN93 in a dose-dependent manner (Fig. 4, A and B). Nifedipine, which was administered at concentrations greater than those of efonidipine, did not affect secretion of either aldosterone or cortisol (Fig. 4, A and B). Moreover, dnNRSF-induced increases in hCYP11B2 and hCYP11B1 mRNAs were suppressed by efonidipine and KN93 but not by nifedipine (Fig. 4, C and D). These data suggest that a T-type calcium channel, probably Cav3.2, is responsible for dnNRSF-induced hCYP11B2 and hCYP11B1 expression.

NRSF/NRSE-mediated transcriptional regulation of rat CACNA1H (rCACNA1H) is involved in aldosterone and corticosterone production in rat adrenal cells

To confirm whether the effect of NRSF/NRSE-mediated steroidogenesis was widely adapted in the other species, we performed similar experiments using in freshly rat isolated adrenal cells. Although rat CYP11B2 (rCYP11B2) and rat CYP11B1 (rCYP11B1) genes do not have NRSEs, aldosterone and corticosterone synthesis were enhanced by AD/dnNRSF in rat adrenal cells due to increased rCYP11B2 and rCYP11B1 mRNA expression (Fig. 5, A–D). rCACNA1H gene has a NRSE (supplemental

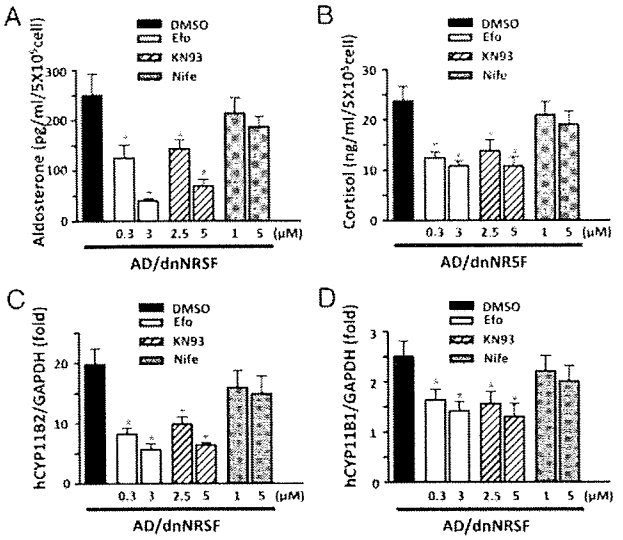

FIG. 4. A T-type calcium channel blocker and a CaMK inhibitor strongly inhibit dnNRSF-induced aldosterone and cortisol secretion by reducing hCYP11B2 and hCYP11B1 mRNA levels in H295R cells. A–D, H295R cells infected with AD/dnNRSF (20 MOIs) were treated with efonidipine (Efo), the CaMK inhibitor KN93, or the L-type calcium channel blocker nifedipine (Nife) in low-serum medium. Aldosterone (A) and cortisol (B) in the culture media were measured as described in *Materials and Methods*. hCYP11B2 (C) and hCYP11B1 mRNA (D) were examined by quantitative RT-PCR. Cells were treated with the drugs at the concentrations indicated for 12 h after the infection. The mean ± SD of four independent experiments is expressed as the fold increase relative to that obtained from cells infected with AD/LacZ (20 MOIs) (C and D). Statistical significance was analyzed using two-way ANOVA. *, $P < 0.05$ *vs.* AD/dnNRSF at 20 MOIs without inhibitor.

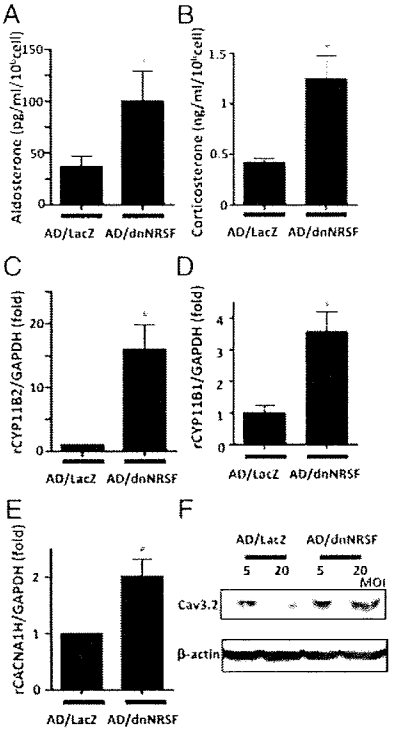

FIG. 5. dnNRSF increases aldosterone and corticosterone synthesis presumably by up-regulating CACNA1H gene expression in rat adrenal cells. A and B, The effect of AD/dnNRSF (20 MOIs) on aldosterone (A) and corticosterone (B) secretion in rat adrenal cells. C and D, rCYP11B2 (C) and rCYP11B1 (D) mRNA were analyzed by quantitative RT-PCR (qRT-PCR) in rat adrenal infected with either AD/LacZ or AD/dnNRSF. E, The induction of rCACNA1H mRNA by forced expression of AD/dnNRSF was analyzed by qRT-PCR in rat adrenal cells. Rat adrenal cells were infected with AD/dnNRSF and AD/LacZ (20 MOIs; A–E). The expression of each mRNA was normalized to that of GAPDH mRNA. The mean ± SD of four independent experiments is expressed as the fold increase relative to that observed in cells infected with AD/LacZ at 20 MOIs. Statistical significance was analyzed using Student's *t* test (*, $P < 0.05$). F, Total cell lysates from rat adrenal cells infected with control AD/LacZ (5 or 20 MOIs) or AD/dnNRSF (5 or 20 MOIs) were subjected to immunoblot analysis with Cav3.2 and β-actin antibodies.

Table 2). As expected, rCACNA1H mRNA was up-regulated by AD/dnNRSF in rat adrenal cells (Fig. 5E), whereas rCACNA1G and rCACNA1C mRNA were not (supplemental Fig. 3, A and B). Increased expression of Cav3.2 in rat adrenal cells was confirmed by immunoblot analysis using a Cav3.2-specific antibody (Fig. 5F). These results suggest that the transcriptional regulation of CACNA1H by NRSF/NRSE is involved in aldosterone and corticosterone synthesis in rat isolated adrenal cells as well as human H295R cells.

NRSF/NRSE system mediates AngII- and K^+-induced increases in hCACNA1H, hCYP11B2, and hCYP11B1 mRNA expression in H295R cells

AngII and K^+ stimulate hCYP11B2 and hCYP11B1 mRNA expression via the calcium-CaM-CaMK pathway (10–12). We investigated NRSF/NRSE-mediated regulation of hCACNA1H, hCYP11B2, and hCYP11B1 gene expression in response to AngII or K^+. In the absence of dnNRSF, the expression of hCACNA1H mRNA was enhanced by AngII (100 nM) and K^+ (10 mM) by approximately 2.4- and 1.9-fold, respectively. However, in the presence of dnNRSF, hCACNA1H expression was generally unaffected (Fig. 6A). Similarly, in the absence of dnNRSF, stimulation with AngII or K^+ increased the expression of the hCYP11B2 gene by 18- and 15-fold, respectively. In the presence of dnNRSF, however, AngII and K^+ increased the hCYP11B2 mRNA by less than 1.5-fold (Fig. 6B). Additionally, in the absence of dnNRSF, stimulation with AngII or K^+ increased the expression of the hCYP11B1 gene by 2.0- and 2.4-fold, respectively, whereas hCYP11B1 mRNA was increased by approximately 1.3-fold in the presence of dnNRSF (Fig. 6C). Collectively, these results suggest that AngII and K^+ augment hCACNA1H, hCYP11B2, and hCYP11B1 mRNA expression through NRSF/NRSE-dependent pathway, at least in part.

Discussion

The present study demonstrates that NRSF/NRSE is involved in aldosterone and cortisol/corticosterone synthesis definitely by regulating CYP11B2 and CYP11B1 gene transcription through NRSF/NRSE-mediated enhancement of CACNA1H gene expression in human H295R and rat adrenal cells and partly by NRSF/NRSE-mediated direct enhancement of CYP11B2 and CYP11B1 gene transcription in human H295R cells.

Among the key molecules in aldosterone and cortisol/corticosterone synthesis, hCYP11B2, hCYP11B1, and hCACNA1H genes have NRSE-like sequences in their transcriptional regulatory regions. However, in a number of other mammalian species including rats, only the CACNA1H gene has a NRSE-like sequence. In the present study, AD/dnNRSF increased expression

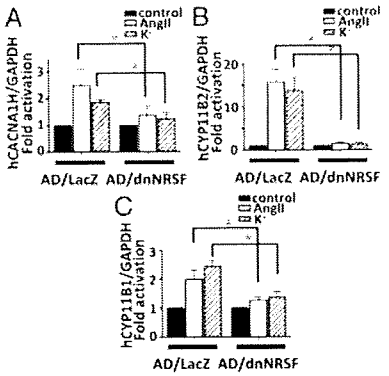

FIG. 6. Inhibition of NRSF contributes to AngII- and K^+-induced increases in hCACNA1H, hCYP11B2, and hCYP11B1 gene expression in H295R cells. A–C, AD/LacZ and AD/dnNRSF (20 MOIs)-infected H295R cells were stimulated by AngII (100 nM) or K^+ (10 mM) for 12 h in low-serum medium, and the effect on hCACNA1H (A), hCYP11B2 (B), and hCYP11B1 (C) mRNA expression was measured. The mean ± SD of five independent experiments is expressed as the fold activation relative to that observed in cells transfected with each AD. Statistical significance was analyzed using two-way ANOVA (*, $P < 0.05$).

of CYP11B2 and CYP11B1 mRNA and augmented secretion of aldosterone and cortisol/corticosterone in both human H295R cells and rat adrenal cells, clearly indicating that NRSF/NRSE indirectly regulates CYP11B2 and CYP11B1 gene expression. NRSF/NRSE increases expression of the CACNA1H gene in mouse cardiomyocytes, and NRSF binds to the NRSE in the CACNA1H gene by EMSA (23). In the present study, AD/dnNRSF augmented CACNA1H mRNA. Given that calcium influx through Cav3.2 calcium channels augments CYP11B2 and CYP11B1 gene transcription through the CaM-CaMK-dependent pathway, it is likely that NRSF/NRSE-mediated enhancement of CACNA1H gene expression leads to up-regulation of CYP11B2 and CY11B1 mRNA in human H295R cells and rat adrenal cells. The repressor effect of $NRSE^{B2}$ and $NRSE^{B1}$ on reporter genes driven by hCYP11B2 and hCYP11B1 promoters is less than 40%; thus, NRSF/NRSE regulates hCYP11B2 and hCYP11B1 gene transcription mainly through the indirect pathway. However, in reporter gene analyses, EMSA and ChIP assay of human H295R cells reveals that NRSF/NRSE system directly regulates transcription of hCYP11B2 and hCYP11B1.

AngII and extracellular K^+ stimulate aldosterone and cortisol synthesis by inducing expression of CYP11B2 and CYP11B1. AngII and K^+ also induce expression of several types of calcium channels including T-type calcium channels (9). These stimuli increase intracellular calcium and trigger CaM-CaMK signaling. In fact, we recently reported that a dual T/L-type calcium channel blocker dose-dependently inhibits AngII- or K^+-induced aldosterone and cortisol secretion (9). However, it is not fully understood how AngII and K^+ induce CYP11B2 and CYP11B1 gene expression. In this study, we have demonstrated that AngII- or K^+-induced expression of CACNA1H mRNA (Cav3.2) is regulated by the NRSF/NRSE system. Thus, induction of CaM-CaMK via calcium influx through T-type calcium channels may partially account for AngII- or K^+-induced aldosterone and cortisol synthesis.

The NRSEs that exist in the intron-exon boundary function as suppressor elements. Several *cis*-acting enhancer elements of the hCYP11B2 gene, including cAMP response element, nerve growth factor-induced clone B response element-1, and Adrenal 5, have been identified in the 5′-flanking region of the hCYP11B2 gene (13–15). NRSE might be the first suppressor element that functions within the hCYP11B2 and hCYP11B1 genes.

The repressor function of the NRSF/NRSE system on gene regulation might be generally ineffective in HF patients. Aldosterone is a clinical marker of HF and AngII is also increased in HF. The increase in both aldosterone and AngII reflects a compensatory response in tissue and systemic renin-angiotensin systems. AngII might cancel the suppressor activity of NRSF in aldosterone synthesis. Previously we demonstrated that NRSF/NRSE system mediates the induction of fetal cardiac genes in cardiomyocytes in response to hypertrophic stimuli (21, 22). Mice overexpressing dnNRSF in cardiomyocytes exhibit cardiac phenotypes that resemble dilated cardiomyopathy, and they die of fatal ventricular arrhythmia. Consistently, NRSE-containing genes, such as atrial natriuretic peptides, B-type natriuretic peptides, and α-skeletal actin are all up-regulated in HF. These cancelation of the NRSF/NRSE system might modify the pathophysiological conditions in the HF.

It is unknown how NRSE-mediated repression of NRSE-containing genes (CACNA1H, CYP11B2, and CYP11B1) is regulated. Given that NRSF recruits mSin3 as well as class I and class II histone deacetylase complexes to repress gene transcription (29, 30), it is likely that NRSF represses these genes using similar mechanisms. It is also unclear how AngII and K^+ cancel the NRSE-mediated repression. Neither AngII nor K^+ down-regulates NRSF mRNA or protein expression (supplemental Fig. 4). Therefore, the lack of NRSF/NRSE-mediated suppression cannot be ascribed to a reduction of NRSF. Endothelin or outside-in fibronectin signaling inhibits the binding of NRSF to NRSEs in cultured cardiomyocytes (22). The contribution of this mechanism and the significance of species-specific presence of NRSE in hCYP11B2 and hCYP11B1 genes require further clarification. However, in the present study, we report a novel role of NRSF/NRSE system in aldosterone and cortisol/corticosterone production in human and rat adrenocortical cells (supplemental Fig. 5).

Acknowledgments

Address all correspondence and requests for reprints to: Yoshihiko Saito, The First Department of Internal Medicine, Nara Medical University, 840 Shijo-cho, Kashihara, Nara 634, Japan. E-mail: yssaito@naramed-u.ac.jp.

This work was supported by research grants from the Japanese Ministry of Education, Science, and Culture and the Japanese Ministry of Health and Welfare.

Disclosure Summary: The authors have nothing to disclose.

References

1. Packer M 1992 The neurohormonal hypothesis: a theory to explain the mechanism of disease progression in heart failure. J Am Coll Cardiol 20:248–254
2. Struthers AD 2004 Aldosterone-induced vasculopathy. Mol Cell Endocrinol 217:239–241
3. Güder G, Bauersachs J, Frantz S, Weismann D, Allolio B, Ertl G, Angermann

CE, Störk S 2007 Complementary and incremental mortality risk prediction by cortisol and aldosterone in chronic heart failure. Circulation 115:1754–1761
4. Mornet E, Dupont J, Vitek A, White PC 1989 Characterization of two genes encoding human steroid 11β-hydroxylase [P-450(11)β]. J Biol Chem 264: 20961–20967
5. Curnow KM, Tusie-Luna MT, Pascoe L, Natarajan R, Gu JL, Nadler JL, White PC 1991 The product of the CYP11B2 gene is required for aldosterone biosynthesis in the human adrenal cortex. Mol Endocrinol 5:1513–1522
6. Aguilera G, Catt KJ 1986 Participation of voltage-dependent calcium channels in the regulation of adrenal glomerulosa function by angiotensin II and potassium. Endocrinology 118:112–118
7. Bird IM, Mathis JM, Mason JI, Rainey WE 1995 Ca(2+)-regulated expression of steroid hydroxylases in H295R human adrenocortical cells. Endocrinology 136:5677–5684
8. Koritz SB 1986 The stimulation by calcium and its inhibition by ADP of cholesterol side-chain cleavage activity in adrenal mitochondria. J Steroid Biochem 24:569–576
9. Imagawa K, Okayama S, Takaoka M, Kawata H, Naya N, Nakajima T, Horii M, Uemura S, Saito Y 2006 Inhibitory effect of efonidipine on aldosterone synthesis and secretion in human adrenocarcinoma (H295R) cells. J Cardiovasc Pharmacol 47:133–138
10. Pezzi V, Clyne CD, Ando S, Mathis JM, Rainey WE 1997 Ca(2+)-regulated expression of aldosterone synthase is mediated by calmodulin and calmodulin-dependent protein kinases. Endocrinology 138:835–838
11. Condon JC, Pezzi V, Drummond BM, Yin S, Rainey WE 2002 Calmodulin-dependent kinase I regulates adrenal cell expression of aldosterone synthase. Endocrinology 143:3651–3657
12. Wilson JX, Aguilera G, Catt KJ 1984 Inhibitory actions of calmodulin antagonists on steroidogenesis in zona glomerulosa cells. Endocrinology 115:1357–1363
13. Bassett MH, Suzuki T, Sasano H, White PC, Rainey WE 2004 The orphan nuclear receptors NURR1 and NGFIB regulate adrenal aldosterone production. Mol Endocrinol 18:279–290
14. Kurihara I, Shibata H, Kobayashi S, Suda N, Ikeda Y, Yokota K, Murai A, Saito I, Rainey WE, Saruta T 2005 Ubc9 and protein inhibitor of activated STAT 1 activate chicken ovalbumin upstream promoter-transcription factor I-mediated human CYP11B2 gene transcription. J Biol Chem 280:6721–6730
15. Clyne CD, Zhang Y, Slutsker L, Mathis JM, White PC, Rainey WE 1997 Angiotensin II and potassium regulate human CYP11B2 transcription through common *cis*-elements. Mol Endocrinol 11:638–649
16. Bassett MH, Zhang Y, Clyne C, White PC, Rainey WE 2002 Differential regulation of aldosterone synthase and 11β-hydroxylase transcription by steroidogenic factor-1. J Mol Endocrinol 28:125–135
17. Wang XL, Bassett M, Zhang Y, Yin S, Clyne C, White PC, Rainey WE 2000 Transcriptional regulation of human 11β-hydroxylase (hCYP11B1). Endocrinology 141:3587–3594
18. Schoenherr CJ, Anderson DJ 1995 The neuron-restrictive silencer factor (NRSF): a coordinate repressor of multiple neuron-specific genes. Science 267: 1360–1363
19. Mori N, Schoenherr C, Vandenbergh DJ, Anderson DJ 1992 A common silencer element in the SCG10 and type II Na+ channel genes binds a factor present in nonneuronal cells but not in neuronal cells. Neuron 9:45–54
20. Chong JA, Tapia-Ramírez J, Kim S, Toledo-Aral JJ, Zheng Y, Boutros MC, Altshuller YM, Frohman MA, Kraner SD, Mandel G 1995 REST: a mammalian silencer protein that restricts sodium channel gene expression to neurons. Cell 80:949–957
21. Kuwahara K, Saito Y, Ogawa E, Takahashi N, Nakagawa Y, Naruse Y, Harada M, Hamanaka I, Izumi T, Miyamoto Y, Kishimoto I, Kawakami R, Nakanishi M, Mori N, Nakao K 2001 The neuron-restrictive silencer element-neuron-restrictive silencer factor system regulates basal and endothelin 1-inducible atrial natriuretic peptide gene expression in ventricular myocytes. Mol Cell Biol 21:2085–2097
22. Ogawa E, Saito Y, Kuwahara K, Harada M, Miyamoto Y, Hamanaka I, Kajiyama N, Takahashi N, Izumi T, Kawakami R, Kishimoto I, Naruse Y, Mori N, Nakao K 2002 Fibronectin signaling stimulates BNP gene transcription by inhibiting neuron-restrictive silencer element-dependent repression. Cardiovasc Res 53:451–459
23. Kuwahara K, Saito Y, Takano M, Arai Y, Yasuno S, Nakagawa Y, Takahashi N, Adachi Y, Takemura G, Horie M, Miyamoto Y, Morisaki T, Kuratomi S, Noma A, Fujiwara H, Yoshimasa Y, Kinoshita H, Kawakami R, Kishimoto I, Nakanishi M, Usami S, Saito Y, Harada M, Nakao K 2003 NRSF regulates the fetal cardiac gene program and maintains normal cardiac structure and function. EMBO J 22:6310–6321
24. Lotshaw DP 2001 Role of membrane depolarization and T-type Ca2+ channels in angiotensin II and K+ stimulated aldosterone secretion. Mol Cell Endocrinol 2175:157–171
25. Chen XL, Bayliss DA, Fern RJ, Barrett PQ 1999 A role for T-type Ca2+ channels in the synergistic control of aldosterone production by ANG II and K+. Am J Physiol 276:F674–F683
26. Gazdar AF, Oie HK, Shackleton CH, Chen TR, Triche TJ, Myers CE, Chrousos GP, Brennan MF, Stein CA, La Rocca RV 1990 Establishment and characterization of a human adrenocortical carcinoma cell line that expresses multiple pathways of steroid biosynthesis. Cancer Res 50:5488–5496
27. Gallo-Payet N, Chouinard L, Balestre MN, Guillon G 1991 Involvement of protein kinase C in the coupling between the V1 vasopressin receptor and phospholipase C in rat glomerulosa cells: effects on aldosterone secretion. Endocrinology 129:623–634
28. Chen ZF, Paquette AJ, Anderson DJ 1998 NRSF/REST is required *in vivo* for repression of multiple neuronal target genes during embryogenesis Nat Genet 20:136–142
29. Andrés ME, Burger C, Peral-Rubio MJ, Battaglioli E, Anderson ME, Grimes J, Dallman J, Ballas N, Mandel G 1999 CoREST: a functional corepressor required for regulation of neural-specific gene expression. Proc Natl Acad Sci USA 96:9873–9878
30. Roopra A, Sharling L, Wood IC, Briggs T, Bachfischer U, Paquette AJ, Buckley NJ 2000 Transcriptional repression by neuron-restrictive silencer factor is mediated via the Sin3-histone deacetylase complex. Mol Cell Biol 20:2147–2157

Circ J 2009; **73:** 1674–1682

Treatment With Recombinant Placental Growth Factor (PlGF) Enhances Both Angiogenesis and Arteriogenesis and Improves Survival After Myocardial Infarction

Yukiji Takeda, MD; Shiro Uemura, MD; Hajime Iwama, MD; Kei-ichi Imagawa, MD; Taku Nishida, MD; Kenji Onoue, MD; Yasuhiro Takemoto, MD; Tsunenari Soeda, MD; Satoshi Okayama, MD; Satoshi Somekawa, MD; Ken-ichi Ishigami, MD; Minoru Takaoka, MD; Hiroyuki Kawata, MD; Atsushi Kubo, MD; Manabu Horii, MD; Tamio Nakajima, MD; Yoshihiko Saito, MD

Background: Placental growth factor (PlGF), a homolog of vascular endothelial growth factor, is reported to stimulate angiogenesis and arteriogenesis in pathological conditions. It was recently demonstrated that PlGF is rapidly produced in myocardial tissue during acute myocardial infarction (MI). However, the effects of exogenous PlGF administration on the healing process after MI are not fully understood. The purpose of the present study was to examine whether PlGF treatment has therapeutic potential in MI.

Methods and Results: Recombinant human PlGF (rhPlGF: 10μg) was administered continuously for 3 days in a mouse model of acute MI. rhPlGF treatment significantly improved survival rate after MI and preserved cardiac function relative to control mice. The numbers of CD31-positive cells and α-smooth muscle actin-positive vessels in the infarct area were significantly increased in the rhPlGF group. Endothelial progenitor cells (Flk-1$^+$Sca-1$^+$ cells) were mobilized by rhPlGF into the peripheral circulation. Furthermore, rhPlGF promoted the recruitment of GFP-labeled bone marrow cells to the infarct area, but only a few of those migrating cells differentiated into endothelial cells.

Conclusions: Exogenous PlGF plays an important role in healing processes by improving cardiac function and stimulating angiogenesis following MI. It can be considered as a new therapeutic molecule. (*Circ J* 2009; **73:** 1674–1682)

Key Words: Myocardial infarction; Placental growth factor; Soluble Flt-1

In patients with acute myocardial infarction (AMI), reperfusion of the occluded coronary artery is of great importance in salvaging ischemic myocardium and minimizing ventricular infarct size. Although reperfusion therapy has contributed to approximately 30% decline in the mortality rate of AMI over the past decade, the rate of rehospitalization because of congestive heart failure that occurs as a result of left ventricular dysfunction with myocardial infarction (MI) is still high.[1] To improve both the cardiac function and the prognosis of patients with AMI, several adjunctive therapies using cell transplantation[2,3] and some growth factors[4,5] have been tried clinically in the past decade. Lunde et al reported that intracoronary injection of autologous mononuclear bone marrow cells (BMCs) had no effect on AMI over a 6-month follow-up.[6] Although gene therapy using vascular endothelial growth factor (VEGF) has successfully induced angiogenesis in rodent models by mobilizing endothelial progenitor cells (EPCs) to the peripheral circulation, there are few reports that VEGF has improved cardiac function in patients with ischemic heart diseases.[7,8] Adjunctive therapies, therefore, have not yet demonstrated an improvement in the clinical prognosis of AMI.

Placental growth factor (PlGF), a homolog of VEGF, is reported to stimulate angiogenesis and arteriogenesis[9–11] with an efficacy at least comparable to that of VEGF, but without any of the side-effects that normally accompany VEGF therapy, such as edema, hypotension,[12] and hemangioma-genesis. We have recently demonstrated that PlGF is produced rapidly in infarcted myocardial tissue, and that the plasma level of PlGF after MI is positively correlated with the improvement in left ventricular function in patients with AMI.[13] These findings suggest that PlGF is involved in post-AMI pathology, infiltration of inflammatory cells, neoangiogenesis, and the development of fibrosis and thus the healing process after AMI. However, therapeutic effects of PlGF administration have not been studied, so in the present study we investigated the result of exogenous administration of PLGF protein in regard to cardiac function and prognosis after MI.

(Received November 19, 2008; revised manuscript received March 30, 2009; accepted April 21, 2009; released online July 15, 2009)

First Department of Internal Medicine, Nara Medical University, Kashihara, Japan
Mailing address: Shiro Uemura, MD, First Department of Internal Medicine, Nara Medical University, 840 Shijocho, Kashihara 634-8522, Japan. E-mail: suemura@naramed-u.ac.jp

Methods

Preparation of Recombinant Human PlGF (rhPlGF)

A DNA sequence encoding the mature human PlGF protein[14] (amino acid residues 21–149 of the 149-amino acid form of PlGF) was amplified by polymerase chain reaction (PCR) with human placental cDNA (TaKaRa, Ohtsu, Japan) as a template. *Escherichia coli* BL21 was transformed with the expression vector, and the thioredoxin-PlGF fusion protein was expressed and purified essentially as previously described.[15] Proteins were concentrated and suspended in a solution containing 20 mmol/L PB (pH 7.4), 0.5 mol/L NaCl, 1 mmol/L dithiothreitol, and 8 mol/L urea, and purified by HisTrap FF (GE Healthcare Bio-Sciences, Piscataway, NJ, USA) column chromatography. Following dialysis against graded concentrations of urea containing 50 mmol/L Tris-HCl (pH 8.0), the fusion protein was resuspended in 50 mmol/L Tris-HCl (pH 8.0). After digestion by EKMax Enterokinase (Invitrogen, Carlsbad, CA, USA), proteins were suspended again in a solution containing 1 mmol/L dithiothreitol and 8 mol/L urea and applied onto a HisTrap FF column in order to remove the tag protein. The purified PlGF was dialyzed against graded concentrations of urea containing 20 mmol/L Tris-HCl (pH 8.0). Finally, the protein solution was fractionated by gel filtration on a Superdex 75 10/300GL column (GE Healthcare Bio-Sciences).

Preparation of Recombinant Human Soluble Flt-1 (rhsFlt-1)

A DNA fragment encoding amino acids 1–338 of human Flt1 (sFlt1 (D1-3) containing 3 Ig-like domains at the N-termini was amplified by PCR reaction with specific primers (forward primer: 5'-CATCCATGGATCCTGAACTGAGTTTAAAAG-3', reverse primer: 5'-CATGGATCCTCAATGTTTCACAGTGATGAATGC-3') and human placental cDNA (Clontech) as a template. The expression vector was used for transformation of BL21 star (CE3) competent cells (Invitrogen). For bacterial expression, the transformant expressing sFlt1 (D1-3) was cultured in LB medium containing 50μg/ml of Kanamycin at 37°C. Four hours after IPTG was added to the final concentration of 1 mmol/L, the cells were collected by centrifuge. The cells were lysed by incubation with 2 mg/ml Lysozyme and sonication. Inclusion bodies were collected by centrifuging for 20 min at 10,000 rpm, and were suspended and solubilized in 20 mmol/L PB containing 0.5 mol/L NaCl, 6 mol/L urea, 1 mmol/L DTT, and 20 mmol/L imidazole followed by His-Trap FF (GE Healthcare Bio-Sciences) column purification. Elute was dialyzed against a graded concentration of urea in 20 mmol/L Tris (pH 8.0) containing 0.5 mol/L NaCl. Following the final dialysis against 20 mmol/L Tris (pH 8.0) containing 0.5 mol/L NaCl, purified sFlt-1 was harvested.

Animals

C57BL/6 mice were purchased from SLC (Shizuoka, Japan). Transgenic mice (C57BL/6 background) that ubiquitously express enhanced GFP (GFP mice) were a generous gift from Dr Masaru Okabe (Osaka University, Suita, Japan). All experimental procedures were performed in accordance with protocols approved by the Ethics Review Committee for Animal Experimentation of Nara Medical University.

Preparation of Mouse Model of MI

C57BL/6 mice (12 weeks old) were anesthetized with diethyl ether inhalation and an osmotic minipump (Durect Corp, Cupertino, CA, USA) filled with 10μg of rhPlGF or 40μg of rhsFlt-1 was implanted subcutaneously. A polyethylene tube connected to the osmotic minipump was extended to the peritoneal cavity and stitched to the oblique abdominal muscle using a 7-0 silk suture. The next day, coronary ligation was performed in the same mouse, as previously reported.[13,16] rhPlGF was infused for 3 days and rhsFlt-1 was infused for 7 days. In total, 95 mice were used for assessing survival rate and 74 mice for histological, physiological and biochemical analyses.

Bone Marrow Transplantation (BMT)

BMT was performed as described previously.[16] Six weeks after BMT, the mice were treated with rhPlGF (10μg) and coronary ligation was performed. Five days after AMI, peripheral blood was collected for fluorescence-activated cell sorting analysis, and hearts were harvested for immunohistochemical examination.

Enzyme-Linked Immunosorbent Assay (ELISA)

Levels of human and murine PlGF were measured by ELISA (R&D System, Germany). The assay for human PlGF recognizes recombinant and natural human PlGF, but not murine PlGF. Murine PlGF also reacts only with natural murine PlGF. Both human and murine PlGF assays recognize free PlGF, but not PlGF bound to sFlt-1.

Binding Assay of rhPlGF With rhsFlt-1 In Vitro

To confirm whether rhsFlt-1 binds to PlGF, we performed an in vitro binding assay. rhsFlt-1, which contains a histidine-tag, was diluted with a solution consisting of 20 mmol/L imidazole, 0.5 mol/L NaCl, 20 mmol/L Tris, and 0.1 mg/ml bovine serum albumin (BSA), at 5 concentrations: 1 ng/20μl, 10 ng/20μl, 100 ng/20μl, 1,000 ng/20μl, and 10,000 ng/20μl, respectively. The rhsFlt-1 solution was mixed with Ni-agarose gel (Qiagen, Valencia, CA, USA), which can bind sFlt-1 that is histidine-tagged. After centrifugation, the supernatant was removed and rhPlGF solution (10 ng/100μl: 100 mmol/L NaCl, 50 mmol/L Tris, 20 mmol/L imidazole, 0.1 mg/ml BSA) was added to the precipitation including the Ni-agarose-rhsFlt-1 complex. The solution was incubated overnight at 4°C. After centrifugation in order to remove the Ni-agarose-rhsFlt-1 complex bound to rhPlGF, uncombined rhPlGF in the supernatant was measured by ELISA.

Reverse Transcriptase-PCR

The apex of the infarcted heart was homogenized and RNA was extracted using Trizol reagent (Life Technologies, Grand Island, NY, USA). Reverse transcription was performed and PCR was then conducted using ABI Prism7700 (Applied Biosystems, Carlsbad, CA, USA). The level of brain natriuretic peptide (BNP) in infarcted hearts was detected using Taqman Gene Expression Assays (Applied Biosystems).

Evaluation of Infarct Size

In order to evaluate infarct size, TTC (2,3,5-triphenyltetrazolium chloride; Sigma Chemical Co, St Louis, MO, USA) staining was performed. At 7 or 28 days after coronary ligation, the hearts were excised, washed with phosphate-buffered saline (PBS), and the ventricles were cut into transverse slices. The slices were placed on a culture plate, stained for 15 min at room temperature with 1.0 ml of 1.5% TTC solution to determine the infarct area, and photo-

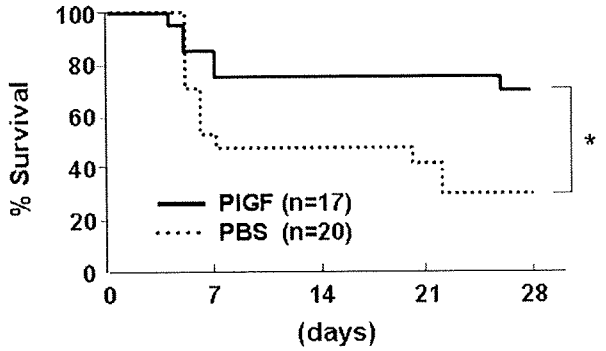

Figure 1. Recombinant human placental growth factor (rhPlGF) protein was produced and administered to C57BL/6 mice. Survival of mice with a myocardial infarct in the rhPlGF group was compared with the phosphate-buffered saline (PBS) group for 28 days after coronary ligation. Values are means±SD; *P<0.05 vs Control.

graphed under a microscope (Olympus Co, Tokyo, Japan). Infarct area and infarct fraction were evaluated. Infarct fraction was calculated as: infarct area/(infarct area+non-infarct area). Fibrin deposition within the infarct area was evaluated by Masson-trichrome staining: areas of fibrin deposition and area of viable tissue were directly measured, and the ratio of fibrin deposition area to viable tissue area (fibrin deposit area/viable tissue area) was calculated. Sequential sections were used to analyze the TTC and Masson-trichrome staining.

Functional Analysis

The left ventricular end-diastolic dimension (LVEDd) and ejection fraction (LVEF) were measured by 2-D guided M-mode echocardiography (Toshiba, Tokyo, Japan).

Immunohistochemistry

The hearts of adult mice were fixed and embedded in frozen sections. The following antibodies were used: anti CD68 antibody (cloneFA-11, UK-Serotec, Oxford, UK), biotin-conjugated monoclonal mouse anti-CD31 antibody (clone390, eBioscience, San Diego, CA, USA), alkaline phosphatase-conjugated anti-α smooth muscle actin (SMA) antibody (clone1A4, Sigma Chemical Co), and Cy3-conjugated anti-αSMA antibody (clone1A4, Sigma Chemical Co).

Statistical Analysis

All results are expressed as the means±SD. Differences between groups were evaluated for statistical significance using Kaplan-Meier analysis, Student's t-test and 1-factor ANOVA. Values of P<0.05 were considered significant.

Results

Recombinant hPlGF Administration and Survival of AMI Mice

The plasma rhPlGF level on the 3rd day of administration by

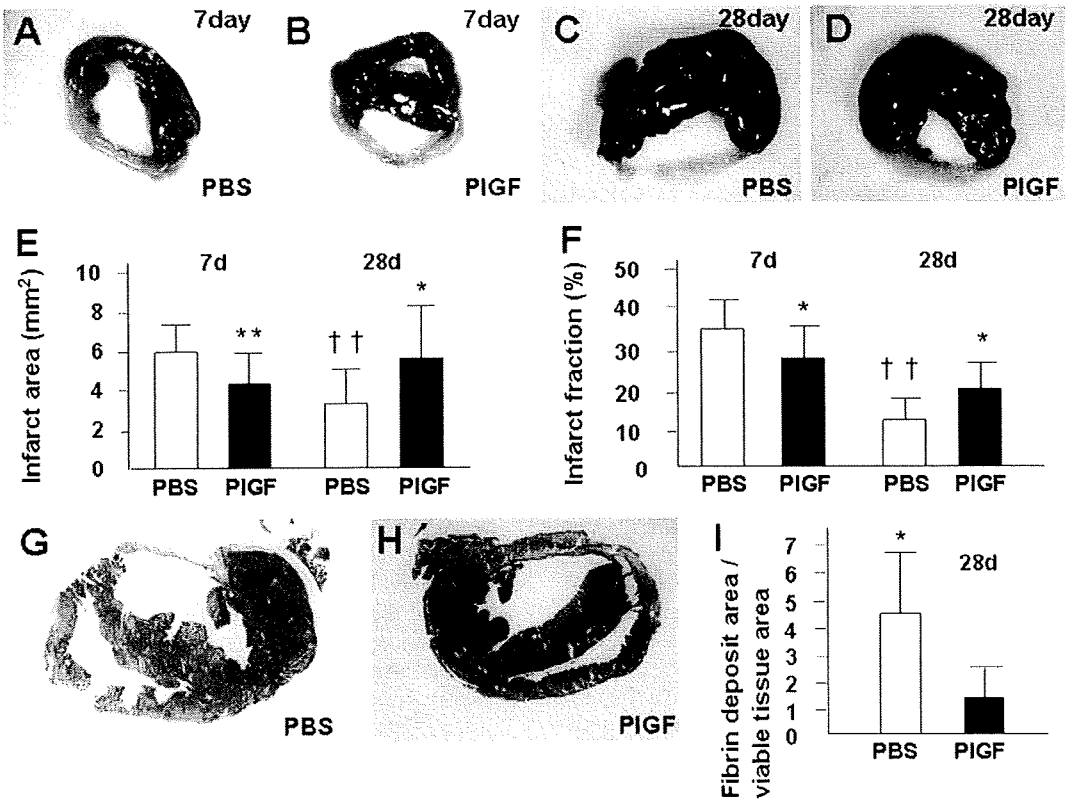

Figure 2. Infarct size and left ventricular function analyzed by TTC staining and echocardiography, respectively. Infarcted hearts of mice treated with both phosphate-buffered saline (PBS) and recombinant human placental growth factor (rhPlGF) were stained with TTC 7 and 28 days after coronary ligation (**A**–**D**). After staining, viable myocardium appeared red and non-viable myocardium appeared white. Infarct area (**E**), and infarct fraction (**F**) were calculated. Representative images of Masson-trichrome staining of a PBS- (**G**) and a rhPlGF- (**H**) treated mouse. The ratio of fibrin deposition area to viable tissue area (fibrin deposit area/viable tissue area) was calculated (**I**). Values are means±SD; *P<0.05, **P<0.01 (comparison between PBS and rhPlGF groups). ††P<0.01 (comparison between the same color bars).